

Cite this: *Chem. Sci.*, 2026, 17, 2413

# Coupled dehydration and hydrogenation catalysis for one-pot conversion of saccharides into high-value furanic compounds

Xiaomeng Cheng,<sup>a</sup> Minghua Dong,<sup>b</sup> Huizhen Liu \*<sup>bc</sup> and Buxing Han \*<sup>bc</sup>

The sustainable conversion of carbohydrates into furanic compounds (e.g., 2,5-dimethylfuran, 2-methylfuran and furfuryl alcohol) through coupled dehydration and hydrogenation represents a pivotal route for biomass valorization. This review systematically summarizes recent advances in catalytic systems enabling the tandem dehydration of carbohydrates and selective hydrogenation of intermediates to target furanic compounds. Key focus areas include the design of multifunctional catalysts (e.g., acid–metal bifunctional sites, porous frameworks), solvent effects, and modulation of reaction pathways to mitigate side reactions. Mechanistic insights into substrate–catalyst interactions, hydrogen transfer dynamics, and stability challenges are critically discussed. Furthermore, techno-economic barriers and scalability of integrated processes are analyzed, highlighting the balance between catalytic efficiency and sustainability. By bridging gaps in fundamental understanding and industrial applicability, this work provides a roadmap for optimizing coupled dehydration–hydrogenation systems to achieve high-yield, energy-efficient furan production from renewable feedstocks.

Received 31st July 2025  
Accepted 3rd January 2026

DOI: 10.1039/d5sc05779e

rsc.li/chemical-science

## 1. Introduction

The increasing urgency to mitigate environmental pollution and the depletion of fossil fuel reserves has made the development and utilization of renewable energy a prominent research

hotspot in recent years.<sup>1,2</sup> Biomass energy, owing to its renewability and abundant reserves, has emerged as an ideal alternative to conventional fossil fuels. Biomass is a renewable carbon resource that can serve not only as a clean energy source but also as a raw material for producing a wide range of high-value chemicals through valorization processes.<sup>3</sup> Lignocellulose, as the most abundant biomass resource, holds great significance in reducing human dependence on fossil fuels by converting it into sustainable chemicals.<sup>4</sup> The intricate composition of lignocellulose, containing hydroxyl, ether, and aldehyde functional groups, provides more opportunities for the sustainable production of oxygenated compounds.<sup>5</sup> As the

<sup>a</sup>School of Ecology and Environment, Zhengzhou University, Zhengzhou, 450001, China

<sup>b</sup>Beijing National Laboratory for Molecular Sciences, CAS Key Laboratory of Colloid and Interface and Thermodynamics, Institute of Chemistry, Chinese Academy of Sciences, Beijing 100190, China

<sup>c</sup>School of Chemistry, University of Chinese Academy of Sciences, Beijing 100049, China



Xiaomeng Cheng

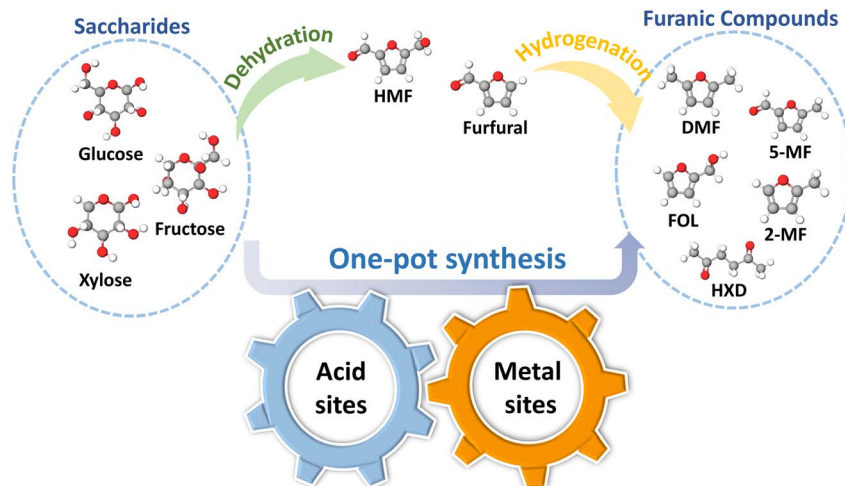
Dr Xiaomeng Cheng received her PhD in Chemistry from Institute of Chemistry, Chinese Academy of Science (CAS) in 2025. She is currently an associate professor at the School of Ecology and Environment, Zhengzhou University. Her research interests now focus on value-added conversion and utilization of biomass-derived compounds.



Minghua Dong

Dr Minghua Dong received his BSc from University of Chinese Academy of Sciences in 2019 and PhD in Physical Chemistry from the Institute of Chemistry, Chinese Academy of Sciences in 2025. He is currently working at Research Institute of Petroleum Processing, SINOPEC, as an assistant researcher. His research interest lies in the catalytic conversion of biomass and computational modelling in heterogenous catalysis.





Scheme 1 Schematic diagram of the synthesis of furanic compounds from saccharides.

key derivatives of lignocellulose, 5-hydroxymethylfurfural (HMF) and furfural can be obtained through the dehydration of cellulose or hemicellulose. These intermediates can subsequently undergo hydrogenation or hydrodeoxygenation (HDO) to yield a range of high-value furanic compounds, providing innovative pathways for green chemistry and sustainable development (Scheme 1).

Furan compounds, including 2,5-dimethylfuran (DMF), 2-methylfuran (2-MF), and 5-methylfurfural (5-MF), are important biomass-derived compounds widely used in biofuels and fine chemicals. For instance, DMF and 2-MF possess energy densities comparable to gasoline, exhibit higher octane numbers and energy densities than ethanol, and demonstrate excellent miscibility with gasoline, and have been extensively studied as important biofuels.<sup>6–8</sup> The traditional production of DMF and other furanic compounds typically involves a two-step process: saccharides are firstly hydrolyzed to HMF or furfural under acid

catalysis, followed by hydrogenation or HDO over metal catalysts to produce furan compounds such as DMF. As a more simplified alternative method, one-pot catalytic processes that integrate dehydration and hydrogenation within a single reactor have attracted widespread attention, since the elimination of intermediate separation and purification steps effectively reduced the operating energy and process complexity.<sup>9,10</sup>

In this review, we provide a comprehensive overview of the catalytic conversion of saccharides into high-value furanic compounds. Particular emphasis is placed on the integration of dehydration and hydrogenation reactions and the design of multifunctional catalysts in tuning catalytic performance. We also discuss recent advances in expanding the substrate scope to include disaccharides and polysaccharides, as well as the challenges and future directions for achieving industrially relevant processes. By addressing these aspects, we aim to



Huizhen Liu

Professor Huizhen Liu received her PhD in Chemistry from the Institute of Chemistry, Chinese Academy of Sciences (CAS) in 2011. She then conducted post-doctoral research at École Polytechnique Fédérale de Lausanne (EPFL), Switzerland (2012–2014), and at Ewha Womans University, South Korea (2014–2015). Since 2015, she has been a full professor at the Institute of Chemistry, CAS. Her research interest currently lies in the catalytic transformation of renewable carbon resources.



Buxing Han

Professor Buxing Han received his PhD (1988) from the Institute of Chemistry, Chinese Academy of Sciences (CAS), and did post-doctoral research (1989–1991) at the University of Saskatchewan. He has been a Professor at the Institute of Chemistry, CAS, since 1993 and is the Chairman of Green Chemistry Committee, Chinese Chemical Society. He works on green chemistry and sustainable chemistry, especially the catalytic transformation of biomass and CO<sub>2</sub> into valuable chemicals. He is an Academician of Chinese Academy of Sciences, a Fellow of the Academy of Sciences for the Developing World (TWAS), and a Fellow of the Royal Society of Chemistry.



contribute to advancing research on the sustainable valorization of saccharides.

## 2. Overview of the hydrolysis and dehydration of saccharides to HMF or furfural and their subsequent hydrogenation

### 2.1 Hydrolysis and dehydration of saccharides

The transformation of saccharides into HMF or furfural involves a sequence of hydrolysis and dehydration reactions. Initially, polysaccharides such as cellulose and hemicellulose are subjected to hydrolysis to yield their respective monosaccharides—glucose from cellulose and xylose from hemicellulose. Once these monosaccharides are obtained, they can be further processed through dehydration reactions. Glucose, owing to its stable pyranose structure, first requires isomerization to fructose under Lewis acid catalysts before dehydration to HMF.<sup>11</sup> In contrast, xylose can be directly dehydrated to furfural in the presence of Brønsted acids.<sup>12</sup> Various catalytic systems have been employed to enhance the activity of the dehydration of saccharides. In homogeneous catalysis, liquid acid catalysts such as inorganic acids (*e.g.*, HCl, H<sub>2</sub>SO<sub>4</sub>) and organic acids (*e.g.*, formic acid, oxalic acid) create an acidic environment that facilitates the reaction.<sup>13–15</sup> However, their corrosive nature and difficulties in recovery pose significant environmental concerns. Meanwhile, metal salt catalysts (*e.g.*, CrCl<sub>3</sub>, FeCl<sub>3</sub>) regulate the reaction pathway by coordinating with saccharides molecules through Lewis acid sites, thereby improving the selectivity toward HMF and furfural.<sup>16</sup> However, the residual metal ions limit the further application. In contrast, numerous heterogeneous solid acid catalysts with Brønsted and Lewis acidic sites have attracted increasing attention in industrial applications due to their recyclability and ease of separation. For instance, sulphonated carbon-based materials have demonstrated high selectivity toward HMF of 91.2% in a DMSO system, but the limited porosity may restrict the diffusion efficiency of saccharide molecules.<sup>17</sup> In comparison, modified zeolites (*e.g.*, SAPO-34) with tunable acidity and well-ordered porous structures efficiently catalyze the dehydration of glucose.<sup>18</sup> Furthermore, metal oxides promote the reaction by introducing mesoporous channels and surface acid sites. Among them, SnO<sub>x</sub>-450 achieves a furfural yield of 53.9% due to the optimized acid site density. However, the high energy consumption associated with the calcination process remains a critical challenge.<sup>19</sup>

Deep eutectic solvents (DESs) have emerged as versatile media for saccharide dehydration due to their tunable hydrogen-bonding networks and inherent Brønsted/Lewis acidity. In ternary formic acid/LiCl DESs, the combined solubilization and dual-acid functions disrupt the hydrogen bonds of cellulose and facilitate glycosidic bond activation, enabling one-pot HMF formation with 60% yield at 180 °C.<sup>20</sup> Acidic DESs also create a highly cooperative environment for fructose conversion when paired with polyoxometalate catalysts. For instance, tetraethyl ammonium chloride (TEAC)–levulinic acid

systems promote efficient dehydration at near-ambient temperature, delivering a HMF yield of 57%.<sup>21</sup> Moreover, the combination of DESs with hierarchical solid acids has also demonstrated promising performance. A representative ChCl/ethylene glycol DES combined with hierarchical porous sulfonated carbon acids (HPCSA) achieves almost complete fructose conversion and HMF yields exceeding 90% at 70 °C, showing the strong synergy between DES-mediated hydroxyl activation of fructose and improved accessibility to acid sites.<sup>22</sup> DESs can function simultaneously as solvents, reactant activators, and co-catalysts, providing a flexible platform for enabling saccharide dehydration.

Ionic liquids, composed of cations and anions in a molten-salt form, offer structural tunability that enables the incorporation of Brønsted or Lewis acidic functionalities, thereby effectively promoting the hydrolysis and dehydration of carbohydrates to furanic compounds. Dual-core sulfonic acid ionic liquids ([bi-C<sub>3</sub>SO<sub>3</sub>HMIM][CH<sub>3</sub>SO<sub>3</sub>]) paired with MnCl<sub>2</sub> efficiently depolymerize cellulose to HMF.<sup>23</sup> The Brønsted acidity of the ILs drives hydrolysis and dehydration, while Mn<sup>2+</sup> promotes isomerization, enabling a 66.5% HMF yield at 120 °C within 1 h. The scope of ILs catalysis further expanded with the integration of polyoxometalates, where the IL facilitates lignocellulosic fractionation and the POMs accelerate pentose dehydration, achieving a maximum furfural yield of 73.4% from sugarcane bagasse, which surpasses mineral-acid systems.<sup>24</sup> Brønsted-acidic ILs (BAILs) also allow direct one-pot conversion of raw lignocellulosic biomass to furfural by coupling C<sub>5</sub>-polymer hydrolysis with dehydration. Imidazolium-based BAILs show high furfural yields in one-pot conversion from raw biomass, underscoring their potential to simplify process steps and improve the sustainability of furfural production.<sup>25</sup> However, ionic liquids still require improved recyclability, greater water tolerance, and more effective product separation to enable practical furan production.

### 2.2 Hydrogenation of HMF and furfural

Following dehydration, HMF and furfural can be further transformed through selective hydrogenation to obtain high-value derivatives. HMF hydrogenation leads to multiple valuable products, including DMF, 5-MF, 2,5-bis-hydroxymethylfuran (BHMF), and 2,5-dimethyltetrahydrofuran (DMTHF), with their selectivity largely determined by the catalyst system and reaction conditions. In DMF synthesis, noble metal catalysts exhibit high activity. For example, the Pd–UiO-66 catalyst achieves a DMF yield of 92.2% under mild conditions, though the scarcity of noble metals resources could limit the large-scale application.<sup>26</sup> To address this issue, bimetallic catalysts utilize the synergistic effects between noble and non-noble metals, achieving cost reduction alongside improved selectivity. For instance, Co<sub>2</sub>Ni<sub>1</sub>@N<sub>1</sub>C-700 significantly enhances the catalytic performance for HMF hydrogenolysis to DMF through the combined action of Co–Ni alloys and Co–N<sub>x</sub> sites.<sup>27</sup> For BHMF synthesis, requiring precise suppression of C–OH bond hydrogenolysis, Pt- and Cu-based catalysts are widely employed. The Pt/CeO<sub>2</sub>–ZrO<sub>2</sub> catalyst



benefits from the electronic effect provided by the oxidized support, which enhances the selectivity of HMF to BHMF. Meanwhile, Cu/ZnO catalyst, due to its lower hydrogenolysis activity, helps minimize by-product formation, thereby improving BHMF selectivity. The deep hydrogenation product 2,5-bis(hydroxymethyl) tetrahydrofuran (BHMTHF) typically requires higher H<sub>2</sub> pressure and an appropriate catalyst. For instance, Pd/MIL-101(Al)-NH<sub>2</sub> enhances BHMTHF selectivity by regulating the adsorption of intermediates through the MOF structure.<sup>28</sup>

Similarly, furfural can be hydrogenated to form furfuryl alcohol (FOL), an important chemical intermediate, which can be further hydrogenate to tetrahydrofurfuryl alcohol (THFOL) or hydrogenolysis to form 2-methylfuran (2-MF). Noble metal catalysts such as Pt or Ir are widely used for liquid-phase hydrogenation to FOL and 2-MF. For example, the Pt/HT catalyst improves Pt dispersion and enhances C=O and H<sub>2</sub> activation through the LDH support, achieving 99% selectivity of FOL.<sup>29</sup> The Ir/C catalyst can achieve a 2-MF yield of 95%, and the presence of Ir oxides provides abundant acidic sites, which significantly enhances the selectivity of the HDO of furfural.<sup>30</sup> For THFOL synthesis, the Ni-ReO<sub>x</sub>/TiO<sub>2</sub> catalyst exhibits excellent hydrogenation activity.<sup>31</sup> The presence of Re modulates the electronic structure of Ni, which enhances the ability to activate the C-OH bond and thereby improving the selectivity of THFOL. By optimizing catalyst composition and reaction conditions, the hydrogenation pathway can be tailored to maximize the yield of targeted products.

Furfural can undergo selective ring-opening hydrogenolysis to produce linear alcohols such as 1-pentanol, 1,2-pentanediol (1,2-PeD) and 1,5-pentanediol (1,5-PeD). Recent works show that achieving high selectivity for these linear alcohols largely depends on (i) the degrees and sites of initial hydrogenation of the furan ring, (ii) the nature and electronic state of the metal active sites, and (iii) the presence of support functionalities that

facilitate H-spillover and C-O cleavage.<sup>32,33</sup> Tailoring support reducibility and vacancy structure can direct the reaction pathway. For example, modification of Pt-supported reducible metal-oxide catalysts with imidazolium-based ionic liquids was shown to enhance hydrogen spillover on the supports, thereby improving the catalytic hydrogenolysis selectivity of furfuryl alcohol toward 1,2-PeD.<sup>36</sup> The impact of support engineering is further exemplified by Ni/La-substituted CeO<sub>2</sub> catalysts, in which the introduction of La modulates the metal-support electronic interactions, enabling efficient cleavage of the furan ring to produce 1,5-PeD with high selectivity.<sup>37</sup> Controlled introduction of basic sites such as Al(OH)<sub>3</sub> on reversed Cu catalysts markedly enhances the selectivity toward 1,2-PeD from furfural.<sup>38</sup> The improvement arises from a shift in the reaction pathway from methylfuran formation to the ring-opening step, because the basic sites promote a parallel adsorption mode of furfuryl alcohol on the catalyst surface. This adsorption configuration strengthens the interaction of the C-O-C bond with the active sites, thereby facilitating the formation of 1,2-PeD.

### 3. Direct conversion of saccharides to furanic compounds

As summarized in Section 2, hydrogenation of HMF and furfural can produce various valuable furanic compounds, such as BHMF, 5-MF, 5-methylfurfuryl alcohol (MFA), DMF, and 2,5-hexanedione (HXD) derived from HMF, as well as FOL, THFOL and 2-MF derived from furfural. However, studies on the direct conversion of saccharides into furanic compounds still remain limited. Current studies mainly focus on the synthesis of DMF and 2-MF, while exploration of other high-value furanic compounds is still insufficient (Fig. 1). To provide a clearer overview of the current research progress, this section categorizes catalytic strategies and systematically reviews the studies

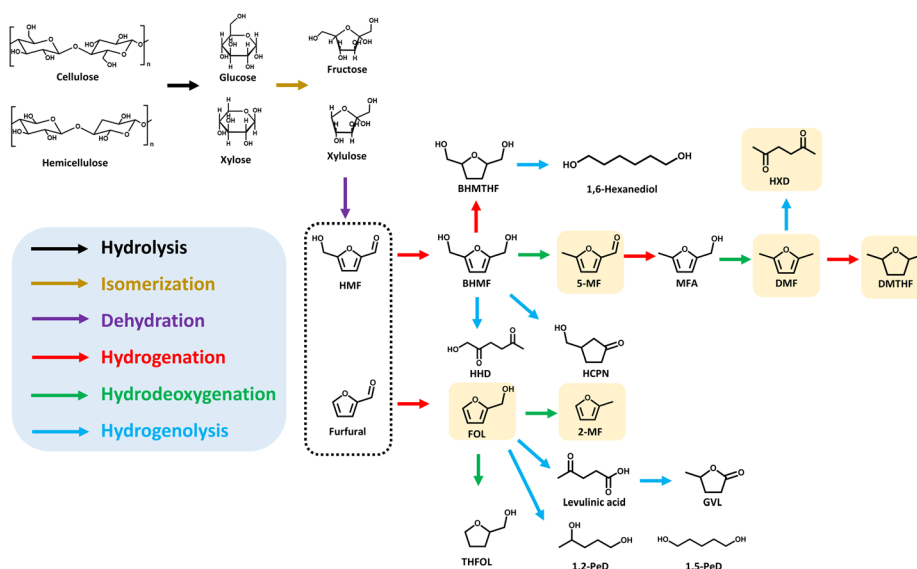


Fig. 1 Possible reaction routes of the transformation of saccharides to different furanic compounds. The yellow highlights represent the furanic compounds that have been reported to be directly converted from saccharides.



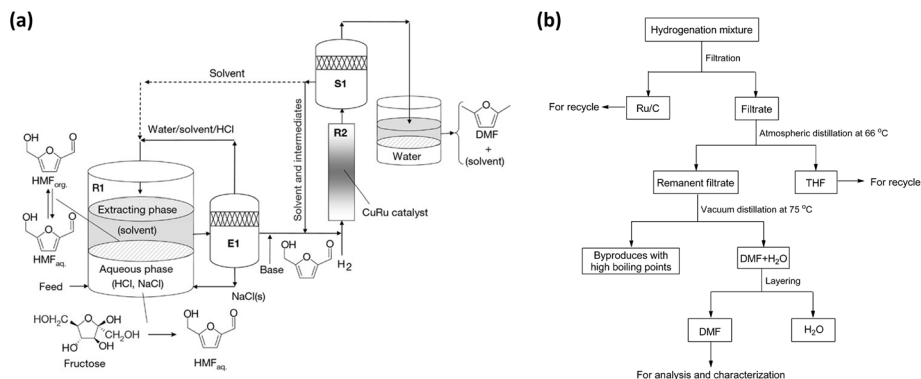


Fig. 2 (a) Schematic diagram of the process for conversion of fructose to DMF. Reprinted with permission from ref. 34. Copyright 2007, Springer Nature; (b) separation of DMF from the hydrogenation mixture. Ref. 35. Copyright 2014, American Chemical Society.

on the direct conversion of saccharides into furanic compounds, ranging from the traditional two-step process requiring intermediate separation to the one-step approach using integrated acid–metal catalysts.

### 3.1 Two-step process

In the tandem reaction of producing furanic compounds from saccharides, a two-step approach was commonly employed in early studies. The first step involved an initial dehydration step using acidic catalysts to generate HMF from hexoses or furfural from pentoses, followed by a separate hydrogenation or hydrogenolysis step in the presence of metal catalysts and a hydrogen source to obtain the desired furanic products. This stepwise approach enabled independent optimization of reaction conditions, including temperature, solvent environment, and active sites. Under this process, the catalytic transformation of hexoses, particularly fructose, into 2,5-dimethylfuran (DMF) represents a key route in the valorization of biomass-derived carbohydrates. A pioneering reaction pathway was proposed by the Dumesic group, which addressed the inherent instability of HMF in aqueous environments by developing a biphasic reactor system.<sup>34</sup> By utilizing HCl in the aqueous phase for fructose dehydration and extracting the intermediate into 1-butanol, followed by vapor-phase hydrogenolysis over a Cu:Ru/C catalyst, a DMF yield of 71% was achieved (Fig. 2a). While this biphasic strategy successfully mitigated humins formation, the reliance on homogeneous acids necessitates corrosion-resistant equipment and neutralization steps, which hinders industrial scalability.

To overcome the limitations of liquid acids, subsequent research shifted toward heterogeneous solid acid catalysts, which offer easier separation and reduced reactor corrosion. For example, Amberlyst-15, a polystyrene-based resin functionalized with surface sulfonic acid groups ( $-\text{SO}_3\text{H}$ ), has demonstrated excellent performance in fructose dehydration. Braun *et al.* developed a two-step catalytic system where Amberlyst-15 facilitated the dehydration of fructose to HMF, followed by a nickel–tungsten–carbide-based catalyst ( $\text{Ni}@/\text{WC}$ ), which facilitated hydrogenation, leading to a DMF yield of 38.5%.<sup>39</sup> In another approach, Amberlyst-15 catalyzed fructose dehydration to achieve a 93% HMF yield, followed by Ru–Sn/

ZnO-catalyzed hydrogenolysis, ultimately delivering a 90% DMF yield in this two-step system.<sup>40</sup> These results suggest that while solid acids such as Amberlyst-15 successfully address corrosion issues, high DMF selectivity remains strongly dependent on noble metals, whereas non-noble systems exhibit limited ability to suppress competing side reactions.

Beyond polymeric resins, carbon-based materials grafted with acidic groups have also shown promise as efficient acid catalysts for saccharides dehydration. For example, cellulose-derived sulfonated carbon catalysts (CCC) functionalized with  $-\text{SO}_3\text{H}$ ,  $-\text{COOH}$ , and  $-\text{OH}$  groups efficiently catalyze saccharide dehydration.<sup>35</sup> The resulting intermediate HMF can be further converted over Ru/C, leading to DMF yields approaching 93%. In this system, ionic liquids/THF biphasic solvent systems are primarily employed to facilitate substrate processing and stabilize dehydration intermediates, but the process still needs solvent switching and multistep separation, increasing operational complexity (Fig. 2b). Although the two-step process allows independent optimization of dehydration and hydrogenolysis catalysts, thereby enabling high yields of furanic compounds, the energy penalty associated with intermediate purification and separation remains a major drawback. Consequently, increasing research efforts have been directed toward integrating these physically separated steps into one-pot catalytic systems.

### 3.2 One-pot process

To overcome the limitations of the two-step method, the one-pot conversion strategy integrates dehydration and subsequent hydrogenation into a single reactor. This method eliminates the need for the isolation and purification of intermediate HMF and furfural, reducing processing time and energy consumption. In this section, the one-pot conversion approach is categorized based on the catalyst system into dual-catalyst systems, where dehydration and hydrogenation are catalyzed by separate functional catalysts, and integrated catalysts that combine both acid and metal sites within a single material.

#### 3.2.1 One-pot process with dual-catalyst systems

**3.2.1.1 Hexose-derived HMF conversion.** One-pot conversion strategies employing dual-catalyst systems have been widely explored to facilitate both saccharide dehydration and



Table 1 One-pot conversion of saccharides to furanic compounds in dual-catalyst systems

| Catalyst   | Substrate   | Product | Reaction conditions  | H source                                       | Conv. (%) | Yield (%) | Ref. |
|--|-------------|---------|--|--|-----------|-----------|------|
| Pd/C + H <sub>2</sub> SO <sub>4</sub>  | Fructose    | DMF     | 150 °C/70 °C, 2 h/15 h, HCOOH/THF  | HCOOH  | —         | 51.0      | 41   |
| Ru/C + AlCl <sub>3</sub> /H <sub>2</sub> SO <sub>4</sub> /H <sub>3</sub> PO <sub>4</sub> | Fructose    | DMF     | 200 °C, 12 h, <i>N,N</i> -DMF  | 1.5 MPa H <sub>2</sub>                         | 99        | 66.3      | 46   |
| Pd/AC + H <sub>2</sub> SO <sub>4</sub>   | Fructose    | DMF     | 130 °C, 12 h, H <sub>2</sub> O-Et <sub>2</sub> O                           | 2.8 MPa H <sub>2</sub>                         | 99.9      | 57.4      | 42   |
|  |             | DMTHF   |  | 2.8 MPa H <sub>2</sub>                         | 99.9      | 69.7      |      |
| Al <sub>2</sub> (SO <sub>4</sub> ) <sub>3</sub> + Pd/C                                   | Cellulose   | HXD     | 200 °C, 1 h, H <sub>2</sub> O-THF  | 2 MPa H <sub>2</sub>                           | 100       | 80.3      | 43   |
| WLC-SO <sub>3</sub> H + Pt <sub>5</sub> Fe <sub>5</sub> /C                               | Fructose    | DMF     | 160 °C/180 °C, 2 h/10 h, 1,4-dioxane-H <sub>2</sub> O                      | 1 MPa N <sub>2</sub> /3 MPa H <sub>2</sub>     | 91.4      | 66.4      | 44   |
| P-UiO-66 + Ni-Co@NC  | Glucose     | DMF     | 160 °C, 8 h, THF-H <sub>2</sub> O  | 0.7 MPa H <sub>2</sub>                         | 98.1      | 82.1      | 52   |
|  | Fructose    |         |  |  | 98.5      | 85.2      |      |
|  | Cellulose   |         |  |  | 83.6      | 63.3      |      |
|  | Starch      |         |  |  | 70.2      | 35.0      |      |
|  | Cellulose   |         |  |  | 65.3      | 20.0      |      |
| NbOPO <sub>4</sub> + Cu-Ru/C   | Fructose    | DMF     | 120 °C/180 °C, WHSV = 0.007 h <sup>-1</sup> , $\gamma$ -butyrolactone      | 5 MPa H <sub>2</sub>                           | 100       | 55.2      | 53   |
| CrCl <sub>2</sub> + NiCl <sub>2</sub>  | L-Rhamnose  | DMF     | 110 °C/0 °C, 2 h/3 h, [Bmim]Cl-MIBK/CH <sub>3</sub> OH                     | NaBH <sub>4</sub>                              | 100       | 91        | 54   |
| NaI  | D-Fructose  | 5-MF    | 210 °C, 7.5 min, toluene/H <sub>2</sub> O                                  | HCOOH  | 100       | 51.0      | 45   |
|  | Glucose     |         |  |  | 100       | 43.5      |      |
|  | Cellulose   |         |  |  | 100       | 39.7      |      |
|  | Corn starch |         |  |  | 100       | 46.0      |      |
| HI-NaI + Pd/C  | Fructose    | 5-MF    | 105 °C/120 °C, 24 h/0.5 h, C <sub>6</sub> H <sub>6</sub> /H <sub>2</sub> O | 2.1 MPa He/2.1 MPa H <sub>2</sub>              | —         | 68        | 55   |
| HI + RhI <sub>3</sub>  | Fructose    | DMTHF   | 125 °C, 14 h, toluene/H <sub>2</sub> O                                     | 2.1 MPa He/2.1 MPa H <sub>2</sub>              | —         | 82        | 56   |
| ZrO <sub>2</sub> -SO <sub>4</sub> + Pt/SiO <sub>2</sub>                                  | Xylose      | FOL     | 130 °C, 6 h, IPA/H <sub>2</sub> O  | 3 MPa H <sub>2</sub>                           | 65        | 33        | 57   |
| Co-N-C   | Xylose      | FOL     | 160 °C, 3 h, 1,4-dioxane/H <sub>2</sub> O                                  | HCOOH  | 100       | 69.5      | 58   |
| H-mordenite + Cu/Fe  | Xylose      | 2-MF    | 260 °C/252 °C, GHSV = 48 h <sup>-1</sup> , toluene/H <sub>2</sub> O        | 0.5 MPa N <sub>2</sub> /0.1 MPa H <sub>2</sub> | 98        | 98        | 59   |
| H- $\beta$ + Cu/ZnO/Al <sub>2</sub> O <sub>3</sub>                                       | Xylose      | FOL     | 190 °C, WHSV = 0.023 h <sup>-1</sup> , GBL/H <sub>2</sub> O                | 0.1 MPa H <sub>2</sub>                         | 99.9      | 87.2      | 60   |
|  |             | 2-MF    |  |  | 99.9      | 86.8      |      |
| H- $\beta$ + NiCu/C  | Xylose      | 2-MF    | 140 °C/220 °C, 5 h/5 h, IPA/H <sub>2</sub> O                               | 4 MPa H <sub>2</sub>                           | 100       | 95.1      | 61   |

subsequent hydrogenation in a single reactor. The performance of catalysts for the one-pot conversion of saccharides to hexose-derived furanic compounds in dual-catalyst systems is summarized in Table 1.

Early studies predominantly used homogeneous acid catalysts combined with supported metal catalysts, which generally afforded high conversion and well-defined reaction pathways. In these systems, strong acids rapidly promote fructose dehydration to HMF, while metal catalysts facilitate subsequent hydrogenolysis or HDO. For instance, Rauchfuss *et al.* reported a formic acid-assisted system in which fructose was dehydrated to HMF in DMSO using H<sub>2</sub>SO<sub>4</sub>, followed by Pd/C-catalyzed hydrogenolysis in THF, achieving a DMF yield of 51.0%.<sup>41</sup> In this system, formic acid acts as both an acid promoter and a hydrogen donor, facilitating transfer hydrogenation without external H<sub>2</sub> (Fig. 3a). Similarly, Liu and co-workers developed a Lewis-Brønsted acid mixture system (AlCl<sub>3</sub>, H<sub>2</sub>SO<sub>4</sub>, and H<sub>3</sub>PO<sub>4</sub>) combined with Ru/C catalyst, achieving a maximum DMF yield of 66.3% from fructose under 1.5 MPa H<sub>2</sub>.<sup>46</sup> The presence of Lewis acidic Al<sup>3+</sup> was shown to promote fructose dehydration, while Ru sites efficiently catalyzed C–O bond cleavage during HDO. Lin *et al.* developed a hydrophilic Brønsted acid catalyst (H<sub>2</sub>SO<sub>4</sub>) and a hydrophobic Pd/AC catalyst in a H<sub>2</sub>O-diethyl ether biphasic tandem catalytic process (biTCP) to convert fructose into DMTHF with a yield of 69.7% (Table 1).<sup>42</sup> Notably, the addition of DMSO selectively poisoned the Pd surfaces, suppressing excessive hydrogenation and

shifting the pathway toward DMF formation, yielding 57.4% DMF (Fig. 3b). This work demonstrates that solvent-induced modulation of metal surface chemistry can be an effective influence on reaction pathways even within homogeneous acid systems. However, the sintering tendency of Pd NPs on the Pd/AC surface under this catalytic process resulted in poor stability. For complex lignocellulosic feedstocks, Al<sub>2</sub>(SO<sub>4</sub>)<sub>3</sub> was acting as a Brønsted acid precursor to hydrolyze cellulose to glucose and dehydrated it to HMF (Fig. 3c).<sup>43</sup> Subsequent hydrogenation and ring-opening over Pd/C yielded 80.3% HXD (Table 1). However, the high activity of homogeneous acids comes at the expense of process sustainability. Corrosivity and catalyst separation remain critical limitations. These drawbacks significantly constrain the industrial relevance of such systems, despite their favorable laboratory-scale performance.

To overcome the drawbacks associated with liquid acids, heterogeneous solid acids have been increasingly employed in combination with metal catalysts to achieve improved stability and tunability. Compared with homogeneous acids, surface-functionalized solid acids generally offer better acidity modulation and recyclability. Importantly, these systems allow more precise tuning of Brønsted *versus* Lewis acid strength, which is critical for balancing fructose dehydration and suppressing undesired condensation reactions. For instance, WLC-SO<sub>3</sub>H, a sulfonated wine lees carbon catalyst, exhibited strong Brønsted acidity while retaining some Lewis acidity, effectively catalyzing fructose dehydration to HMF with a 98.2% yield.<sup>44</sup>



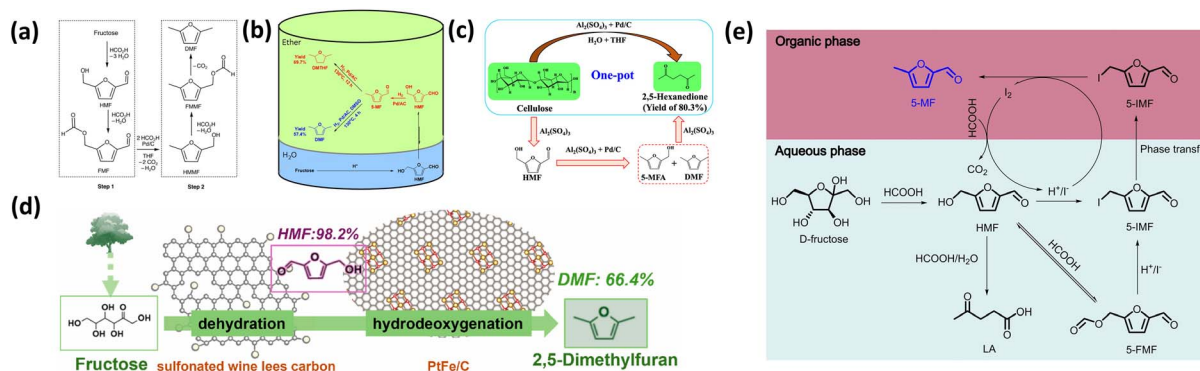


Fig. 3 (a) One-pot process to generate DMF from fructose. Reprinted with permission from ref. 41. Copyright 2010, Wiley; (b) schematic illustration of the conversion of fructose to DMTHF or DMF in a biphasic tandem catalytic process (biTCP). Reprinted with permission from ref. 42. Copyright 2020, ELSEVIER; (c) schematic illustration of the one-pot conversion of cellulose to HXD in  $\text{Al}_2(\text{SO}_4)_3$  and Pd/C catalytic system. Reprinted with permission from ref. 43. Copyright 2023, American Chemical Society; (d) schemes of Fructose conversion on WLC-SO<sub>3</sub>H and PtFe/C catalysts. Reprinted with permission from ref. 44. Copyright 2024, ELSEVIER; (e) possible reaction pathway for the synthesis of 5-MF from D-fructose; Reprinted with permission from ref. 45. Copyright 2021, Wiley.

When combined with Pt<sub>5</sub>Fe<sub>5</sub>/C, a bimetallic catalyst with strong metal-metal interactions and high Lewis acidity, a maximum DMF yield of 66.4% was achieved. Non-noble metal systems have also demonstrated promising activity. Wu *et al.* designed a dual-catalyst system consisting of P-UiO-66 and Ni-Co@NC, achieving a 98.1% conversion of glucose and 82.1% yield of DMF.<sup>52</sup> The Lewis acid Zr<sup>4+</sup> sites in P-UiO-66 facilitated glucose isomerization and dehydration, while the Ni-Co alloy efficiently catalyzed hydrogenation. Importantly, this system exhibited broad substrate tolerance, converting fructose, cellobiose, starch, and cellulose, thereby highlighting the advantages of solid acid-metal systems for processing diverse saccharide feedstocks. The catalytic system composed of niobium phosphate (NbOPO<sub>4</sub>) and Cu-Ru/C was employed for the conversion of fructose to DMF, achieving a maximum DMF yield of 55.2%.<sup>53</sup> The system utilized [Bmim]Cl as a co-catalyst, which activated the hydroxyl groups of fructose through hydrogen bonding to lower the energy barrier of the dehydration reaction. However, the viscosity of high concentration of ILs significantly limited mass transfer and hydrogen diffusion, which in turn constrained the effective utilization of metal sites and restricted the DMF yield.

In addition to acid-metal combinations, halide-based catalytic systems also provide an alternative strategy for modulating reaction pathways in one-pot saccharide conversion. In these systems, halide species, including both inorganic halides and halide-based ionic liquids, actively participate in dehydration and hydrogenation steps rather than merely acting as solvents or additives. Through strong interactions with hydroxyl groups and furan intermediates, halide anions can facilitate C-O bond activation and stabilize key intermediates, thereby enabling reaction routes that differ from conventional acid-catalyzed dehydration followed by metal-catalyzed hydrogenation. CrCl<sub>2</sub> catalyzes the dehydration and cyclization of L-rhamnose to 5-MF in a [Bmim]Cl/MIBK biphasic system, where Cr<sup>2+</sup> acts as a Lewis acid to activate the hydroxyl groups of L-rhamnose.<sup>54</sup> The resulting 5-MF is subsequently converted to DMF *via* a stepwise

reduction and deoxygenation sequence conducted in methanol, involving NaBH<sub>4</sub>-mediated reduction, acetylation, and final Ni<sup>2+</sup>-based deoxygenation, affording a DMF yield of 91% (Table 1). In iodide-mediated systems, fructose is converted to 5-MF with a yield of 51% in a NaI-formic acid medium.<sup>45</sup> The reaction proceeds through sequential dehydration, iodination, and reduction steps involving 5-iodomethylfurfural as an intermediate (Fig. 3e). This strategy is also applicable to starch-derived feedstocks and achieves a productivity of 103 mmol g<sup>-1</sup> h<sup>-1</sup> from corn starch (Table 1). Similarly, Sen and co-workers reported a halide-mediated catalytic system centered on hydroiodic acid (HI).<sup>55</sup> Owing to the dual dehydration-reduction functionality of HI, fructose can be selectively converted to 5-MF *via* HMF and 5-iodomethylfurfural (IMF) intermediates, delivering a 5-MF yield of 68%. The *in situ* regeneration of HI is achieved through metal-catalyzed hydrogenation of I<sub>2</sub>. Building on this strategy, the system was further extended to an HI/RhCl<sub>3</sub> dual-catalyst system, allowing the one-pot conversion of fructose to DMTHF and highlighting the synergistic effects between halide-mediated reaction pathway regulation and metal-catalyzed hydrogenation.<sup>48</sup> These methods utilize halides as both dehydrating and reducing agents, broadening the range of saccharide reaction pathways. However, the presence of halogens inevitably leads to irreversible poisoning of metal active sites and recycling challenges, which increase the cost and complexity of industrial applications.

**3.2.1.2 Pentose-derived furfural conversion.** As the main component of hemicellulose, xylose is a key feedstock for producing high-value pentose-derived furanic compounds. The one-pot conversion of xylose typically involves acid-catalyzed dehydration to furfural, followed by metal-catalyzed hydrogenation to furfuryl alcohol or deep HDO to 2-MF. Compared to conventional two-step processes, one-pot strategies improve atom economy and reduce energy input. However, because the process involves tandem reactions, the main challenge lies in balancing the kinetics of dehydration and hydrogenation while effectively suppressing side reactions, such as the cross-



polymerization of furfural. Fraga and co-workers have developed a bifunctional catalyst system consisting of sulfuric acid-modified  $\text{ZrO}_2$  ( $\text{ZrO}_2\text{-SO}_4$ ) and  $\text{Pt/SiO}_2$ , achieving a 33% yield of FOL.<sup>57</sup> The  $-\text{SO}_3\text{H}$  groups can enhance dehydration activity, though the spatial separation between metal and acid sites allows the highly reactive furfural intermediate to undergo side reactions in the acidic environment while diffusing to the metal site, leading to a low FOL yield.

To improve the coordination between dehydration and hydrogenation steps, several strategic improvements have been explored. An alternative strategy involves replacing molecular hydrogen with catalytic transfer hydrogenation (CTH) to improve hydrogenation efficiency. Using formic acid as both the acid catalyst and hydrogen donor over a non-noble Co–N–C catalyst, Nie *et al.* achieved a FOL yield of 69.5%.<sup>58</sup> This method utilizes *in situ* generated active hydrogen species to accelerate the hydrogenation rate, enabling better matching with the dehydration step and alleviating the adverse effects of stepwise separation in conventional processes. Further advancements in catalyst design, such as the bimetallic 0.5NiCu/C catalyst paired with H-beta zeolite by Ma *et al.* demonstrated the value of bimetallic electronic synergy in product selectivity.<sup>61</sup> The observed high yield of 95.1% for 2-MF confirms that bimetallic structures can selectively promote the C=O bond conversion while suppressing over-hydrogenation of the furan ring and other non-selective side reactions.

Reaction engineering has also provided crucial strategies for intermediate stabilization. An early study utilizing H-mordenite and Cu/Fe in a continuous two-phase plug-flow reactor achieved a high 2-MF yield (98%).<sup>59</sup> Rapid product removal in the continuous flow reactor shortens the residence time of furfural under acidic conditions, reducing its propensity for polymerization. However, the limited stability of H-mordenite under high-temperature and high-pressure conditions poses challenges for further industrial application. Solvent effects also play an important role, as the use of a  $\gamma$ -butyrolactone (GBL)/ $\text{H}_2\text{O}$  mixed solvent stabilizes the furfural intermediate and reduces byproduct formation under acidic conditions.<sup>60</sup> This system also highlighted the potential for temperature-controlled selectivity, allowing the output to be tuned precisely toward FOL (150 °C) or 2-MF (190 °C).

As shown in Table 1, one-pot processes with dual-catalyst systems allow flexible combinations of acidic and metallic functions. Homogeneous acid–metal systems generally promote rapid saccharide dehydration but often require prolonged residence times to complete hydrogenation. In contrast, heterogeneous solid acid–metal systems offer improved catalyst recyclability and broader substrate scope. But the carbon deposition on solid acid surfaces and pore blockage frequently reduces the accessibility of active sites. Halide-mediated systems introduce alternative reaction pathways involving halogenated intermediates, thereby enabling the formation of 5-MF and related products. However, the potential poisoning of metallic sites complicates both reaction kinetics and downstream product purification.

Overall, current dual-catalyst systems mainly rely on condition optimization and functional separation rather than kinetic

synchronization between dehydration and hydrogenation steps. The spatial separation between acid catalytic sites and metal sites forces the dehydration products of saccharides to undergo a mass transfer process before contacting the metal catalyst, which not only prolongs the reaction time but also increases the risk of undesirable byproduct formation. To overcome these problems, researchers have focused on the design of integrated catalysts. By precisely anchoring acidic sites and metal active centers on the same supports, reaction activity can be significantly enhanced through synergistic effects.

### 3.2.2 One-pot process with integrated catalyst systems

**3.2.2.1 Hexose-derived HMF conversion.** One-pot conversion of hexoses to furanic compounds over a single catalyst helps to improve atom economy and process efficiency, but the key challenge is to balance the kinetics of dehydration and hydrogenation while suppressing side reactions such as humin formation and over-hydrogenation. Accordingly, an effective multifunctional catalyst must integrate acidic sites for dehydration with metallic sites for hydrogen activation and transfer within a single catalytic framework. Moreover, the microenvironment provided by the catalyst, such as surface wettability and pore structure, critically influences substrate adsorption, intermediate stabilization, and desorption, thereby directing reaction pathways and product selectivity. Building on these considerations, recent studies have proposed diverse catalyst design strategies to address these challenges (Table 2).

Metal–organic frameworks (MOFs), with their tunable pore structures, high specific surface areas, and abundant active sites, serve as ideal heterogeneous catalyst supports. The rigid and porous frameworks of MOFs provide excellent platforms for constructing multifunctional catalysts that can promote both saccharide dehydration and subsequent hydrogenation reactions. Zr-based MOFs, such as UiO-66, are particularly advantageous for hexose valorization as their inherent Lewis acidic sites facilitate the critical glucose-to-fructose isomerization. A representative example is the Pd/Zr-based UiO-66@sulfonated graphene oxide (Pd/UiO-66@SGO) catalyst, which enables the direct one-pot conversion of fructose and glucose to DMF in yields of 70.5% and 45.3%, respectively.<sup>47</sup> The acidic sites of UiO-66@SGO promote the dehydration of fructose to HMF, while the synergistic effect between UiO-66@SGO and Pd NPs facilitates the subsequent hydrodeoxygenation steps. Moreover, the microporous structure of UiO-66 not only enhances substrate adsorption, but also inhibits excessive hydrogenation by weakening the  $\pi$ – $\pi$  interaction between the furan ring and the SGO graphite surface (Fig. 4a). Building upon this, Kim *et al.* developed bimetallic 10Cu-1Pd/UiO-66( $\text{NH}_2$ )@SGO (10Cu-1Pd/ $\text{U}_{50}\text{S}_{50}$ ) catalyst, which significantly improved DMF yields to 85.1% from fructose and 79.9% from glucose (Table 2).<sup>48</sup> The researchers achieved this by precisely tailoring the distribution of acid sites through varying the ratio of amino-functionalized UiO-66 to SGO. This modulation allowed for an optimal balance between the Lewis acidity of the Zr sites and the Brønsted acidity of the SGO (Fig. 4b). To further overcome mass transfer limitations, the transition to 2D morphologies has proven effective, the Pd/NUS- $\text{SO}_3\text{H}$  nanosheet catalyst achieved a 95.2% DMF yield at 130 °C by providing an open catalytic

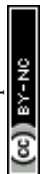


Table 2 One-pot conversion of saccharides to furanic compounds with integrated catalysts

| Catalyst   | Substrate              | Product | Reaction conditions                             | H source                | Conv. (%) | Yield (%) | Ref. |
|--|------------------------|---------|---|-------------------------|-----------|-----------|------|
| 4.8Pd/UiO-66@SGO                                     | Fructose               | DMF     | 160 °C, 3 h, THF                                | 1.0 MPa H <sub>2</sub>  | 91.8      | 70.5      | 47   |
|  | Glucose                |         | 180 °C, 3 h, THF                                |                         | 87.3      | 45.3      |      |
| 10Cu-1Pd/U <sub>50</sub> S <sub>50</sub>             | Fructose               | DMF     | 200 °C, 3 h, THF                                | 1.0 MPa H <sub>2</sub>  | 98.0      | 85.1      | 48   |
|  | Glucose                |         | 200 °C, 3 h, THF                                |                         | 97.0      | 79.9      |      |
|  | Cellobiose             |         | 200 °C, 3 h, THF                                |                         | 90.0      | 67.7      |      |
|  | Sucrose                |         | 200 °C, 3 h, THF                                |                         | 95.0      | 73.4      |      |
|  | Starch                 |         | 200 °C, 6 h, THF                                |                         | 70.0      | 53.6      |      |
|  | Cellulose <sup>a</sup> |         | 200 °C, 6 h, THF                                |                         | 59.0      | 29.8      |      |
| Pd/MIL-53(Al)-P <sup>b</sup>                         | Fructose               | DMF     | 110 °C, 1.25 h, <i>n</i> -BtOH                  | PMHS                    | 99        | 95        | 64   |
|  | Glucose                |         | 130 °C, 2 h, <i>n</i> -BtOH                     |                         | 95        | 54        |      |
|  | Sucrose                |         | 110 °C, 2.5 h, <i>n</i> -BtOH                   |                         | 100       | 73        |      |
|  | Inulin                 |         | 110 °C, 2.5 h, <i>n</i> -BtOH                   |                         | 97        | 86        |      |
|  | Cellulose              |         | 130 °C, 3 h, <i>n</i> -BtOH                     |                         | —         | 32        |      |
| Pd/NUS-SO <sub>3</sub> H                             | Fructose               | DMF     | 150 °C, 24 h, IPA/DMSO                          | 2.0 MPa H <sub>2</sub>  | 100       | 95.2      | 49   |
|  | Glucose                |         | 150 °C, 24 h, IPA/DMSO                          |                         | 100       | 80.8      |      |
|  | Cellobiose             |         | 150 °C, 24 h, IPA/DMSO                          |                         | 100       | 69.9      |      |
|  | Sucrose                |         | 150 °C, 24 h, IPA/DMSO                          |                         | 100       | 68.3      |      |
|  | Inulin                 |         | 150 °C, 24 h, IPA/DMSO                          |                         | 100       | 76.7      |      |
|  | Cellulose              |         | 150 °C, 24 h, IPA/DMSO                          |                         | 100       | 76.7      |      |
| Pd/NUS-PhSO <sub>3</sub> H-Ph                        | Fructose               | DMF     | 100 °C, 6 h, IPA/DMSO                           | PMHS                    | 99.9      | 90.2      | 63   |
|  | Sucrose                |         | 100 °C, 12 h, IPA/DMSO                          |                         | 99.9      | 70.5      |      |
|  | Cellobiose             |         | 100 °C, 24 h, IPA/DMSO                          |                         | 99.9      | 68.5      |      |
|  | Inulin                 |         | 100 °C, 24 h, IPA/DMSO                          |                         | 99.9      | 77.1      |      |
| CuCo@C-TsOH-IM                                       | Fructose               | DMF     | 220 °C, 10 h, THF                               | 3.0 MPa H <sub>2</sub>  | >99       | 71.1      | 66   |
|  | Glucose                |         |   |                         | >99       | 33.7      |      |
|  | Sucrose                |         |   |                         | >99       | 54.2      |      |
|  | Inulin                 |         |   |                         | >99       | 48.3      |      |
|  | Starch                 |         |   |                         | >99       | 44.9      |      |
| Pd/C-SO <sub>3</sub> H-TMS <sup>b</sup>              | Fructose               | DMF     | 120 °C, 1.5 h, <i>n</i> -BuOH                   | PMHS                    | 96        | 92        | 62   |
| Pt/C-S   | Fructose               | DMTHF   | 175 °C, 2 h, EtOH/H <sub>2</sub> O              | 10.3 MPa H <sub>2</sub> | 100       | 50        | 50   |
| C <sub>3</sub> P <sub>1</sub> Z <sub>1</sub> /Y(5.1) | Cellulose              | DMF     | 240 °C, 4 h, scMeOH                             | 2.0 MPa H <sub>2</sub>  | 98.0      | 33.8      | 51   |
|  | Glucose                |         |   |                         | >99       | 39.2      |      |
|  | Sucrose                |         |   |                         | >99       | 35.5      |      |
|  | Starch                 |         |   |                         | 99.0      | 38.5      |      |
|  | Fructose               |         |   |                         | >99       | 41.9      |      |
| Pd/PDVB-S-143  | Fructose               | DMF     | 120 °C, 6 h, <i>n</i> -BuOH                     | PMHS                    | >99       | 94.2      | 65   |
| Pt/ZrO <sub>2</sub> -SO <sub>4</sub>                 | Xylose                 | FOL     | 130 °C, 6 h, IPA/H <sub>2</sub> O               | 3 MPa H <sub>2</sub>    | 32        | 9         | 67   |
| Pt/SBA-15-SO <sub>3</sub> H                          | Xylose                 | FOL     | 130 °C, 6 h, IPA/H <sub>2</sub> O               | 3 MPa H <sub>2</sub>    | 65        | 60        | 71   |
| Cu/SBA-15-SO <sub>3</sub> H                          | Xylose                 | FOL     | 140 °C, 6 h, <i>n</i> -butanol/H <sub>2</sub> O | 4 MPa H <sub>2</sub>    | 93.7      | 63.4      | 68   |
| Beta zeolite   | Xylose                 | FOL     | 130 °C, 1 h, IPA/H <sub>2</sub> O               | 3 MPa H <sub>2</sub>    | —         | 75        | 69   |
| CaCl <sub>2</sub> ·4H <sub>2</sub> O                 | Xylose                 | FOL     | 150 °C, 2 h, IPA/MSH                            | IPA                     | 99.9      | 62        | 70   |

<sup>a</sup> HCl was added as additive. <sup>b</sup> PhCl as additive.

surface that minimizes internal diffusion resistance.<sup>49</sup> This bifunctional catalyst enables a stepwise pathway: HMF is first hydrogenated to BHMF, which undergoes esterification with isopropanol (IPA), followed by hydrogenolysis to yield DMF (Fig. 4c and d). These results indicate that precise control over both the strength and density of acid sites is critical for achieving high selectivity in one-pot hexose conversion.

The main challenge in achieving one-pot conversion with a single catalyst depends on the unavoidable side reactions, such as HMF undergoing irreversible rehydration to form levulinic acid (LA) in the presence of water. To address this issue, extensive research has focused on adjusting the wettability of catalyst surfaces. A promising strategy integrates hydrophobic surface modifications with polymethylhydrosiloxane (PMHS) as a liquid hydrogen donor, creating a hydrophobic microenvironment. This not only protects the furan ring but also

optimizes hydrogen transfer. Mechanistically, this is achieved through a hydrosilylation–hydrogenolysis pathway, where hydrosilylation of the HMF aldehyde group forms a stable silyl ether intermediate that effectively shields the furan ring from water-induced ring-opening reactions. As demonstrated by the Pd/C-SO<sub>3</sub>H-TMS catalyst, synthesized *via* sulfonation of commercial Pd/C followed by trimethylchlorosilane (TMS) treatment, this process efficiently converts fructose to DMF with an 85% yield in *n*-butanol using PhCl as a critical acid additive.<sup>62</sup> The TMS-functionalized surface ensures that Pd<sup>0</sup> metal sites preferentially target the aldehyde and hydroxyl groups, preventing the formation of rehydration byproducts. Furthermore, this concept of wettability control has been extended to 2D framework through the precise tailoring of surface functional groups. As reported by Deng *et al.*, the introduction of hydrophobic *tert*-butylphenyl groups into a sulfonated 2D MOF



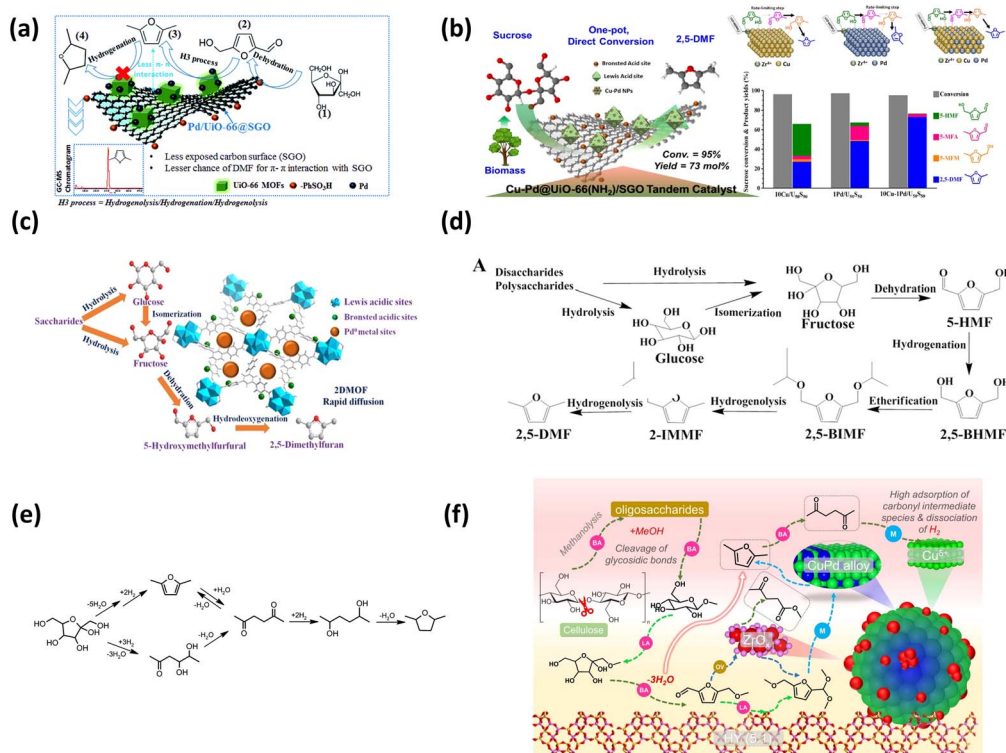


Fig. 4 (a) Schematic illustration of the DMF interaction on the Pd/UiO-66@SGO catalyst surface, the conversion route through a hydrogenolysis–hydrogenation–hydrogenolysis (H3) process, and the corresponding GC-TOF/MS chromatograms. Reprinted with permission from ref. 47. Copyright 2017, Royal Society of Chemistry; (b) plausible transformation of HMF into DMF over the bimetallic Cu-Pd/US catalyst. (i) Sequential fructose dehydration into HMF and direct adsorption of HMF onto the adjacent Cu–Pd metallic phase and (ii) sequential hydrogenation of 5-MFA into 5-MFM and hydrogenolysis of 5-MFM into DMF. Reprinted with permission from ref. 48. Copyright 2019, ELSEVIER. (c) Schematic illustration of Pd/NUS-SO<sub>3</sub>H for one pot conversion of saccharides to DMF and (d) reaction pathway of saccharides and HMF to DMF. Reprinted with permission from ref. 49. Copyright 2022, Wiley. (e) Possible reaction pathways for the hydrodeoxygenation of fructose through the sequential dehydration and hydrogenation steps; Reprinted with permission from ref. 50. Copyright 2015, American Chemical Society. (f) Schematic of cellulose conversion over C<sub>3</sub>P<sub>1</sub>Z<sub>1</sub>/Y(5.1) under scMeOH conditions. Reprinted with permission from ref. 51. Copyright 2024, ELSEVIER.

(Pd/NUS-PhSO<sub>3</sub>H-Ph) allowed for the fine-tuning of surface wettability, which effectively regulated the adsorption–desorption equilibrium of polar furanic intermediates.<sup>63</sup> This engineered microenvironment prevented the localized accumulation of water around the acidic sites, thereby inhibiting the rehydration of HMF and ensuring high DMF selectivity (Table 2).

The broader strategy of utilizing hydrophobic coatings—such as the polydimethylsiloxane (PDMS)-modified Pd/MIL-53(Al)-P,<sup>64</sup> or inherent polymer frameworks like the poly(divinylbenzene) (PDVB)-supported Pd/PDVB-S-143,<sup>65</sup> is to facilitate the rapid desorption of HMF from acidic sites. For instance, the Pd/MIL-53(Al)-P system achieved a 95% DMF yield in chlorobenzene at 110 °C by preventing water accumulation around the active sites. The Pd/PDVB-S-143 catalyst leveraged its organic-friendly matrix to suppress the undesired hydrolysis of both HMF and the final DMF product, while promoting intimate contact between the PMHS donor and furanic reactants. By ensuring a high local H-donor/H<sub>2</sub>O ratio and enhancing interfacial hydrogen transfer, these integrated systems not only achieve exceptional DMF yields at low temperatures (110–130 °

C) but also demonstrate robust performance across diverse feedstocks including glucose, sucrose, and cellulose, effectively bypassing the yield-limiting rehydration to levulinic acid that typically hinders aqueous-phase biomass valorization (Table 2).

The final product distribution can be further diverted toward alternative high-value derivatives or optimized for cost-effectiveness by modulating the metal–support interface. While MOF-based systems offer high selectivity, carbon-supported bimetallic catalysts like CuCo@C-TsOH provide a more economical alternative, achieving a 71.1% DMF yield from fructose while maintaining hydrothermal stability.<sup>66</sup> Conversely, product selectivity can be shifted toward saturated furans or protected intermediates by altering the reaction medium or metal electronic state. Using a sulfur-poisoned Pt/C catalyst intentionally moderates the HDO rate to favor 2,5-dimethyltetrahydrofuran (DMTHF) (47% yield), as the blocked Pt sites prevent the flat adsorption required for furan ring saturation (Fig. 4e).<sup>50</sup> In contrast, the conversion of cellulose over ZrO<sub>2</sub>-doped Cu-Pd/HY in supercritical methanol (scMeOH) proceeds *via* the etherification of HMF into 2,5-bis(methoxymethyl)furan (BMMF), where ZrO<sub>2</sub>-derived oxygen



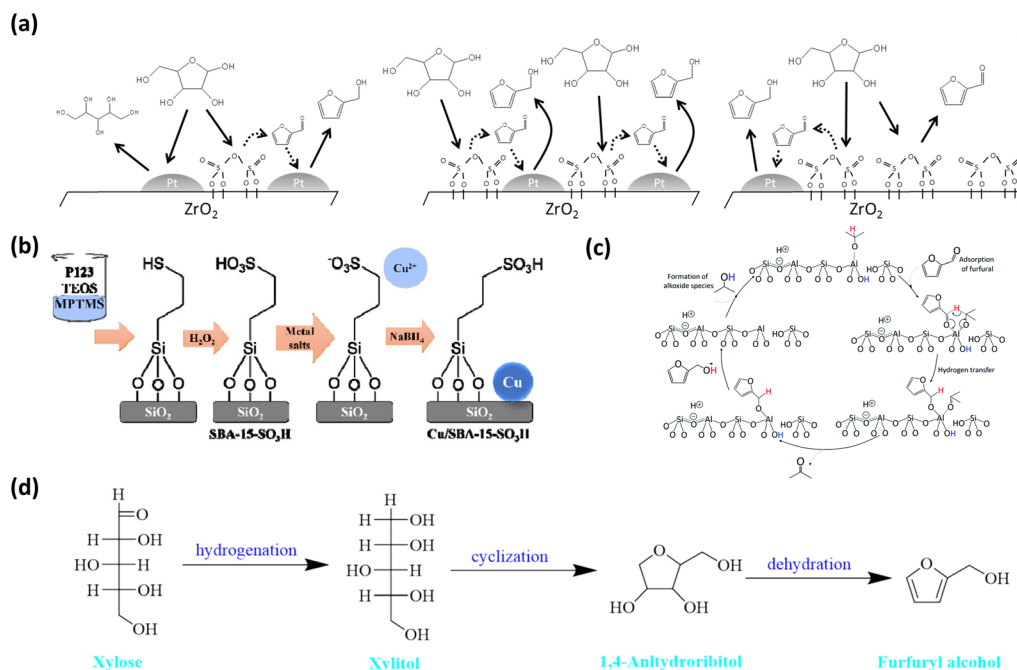


Fig. 5 (a) Pictorial scheme of the surface assembly of Pt/ZrO<sub>2</sub>-SO<sub>4</sub> multifunctional catalysts for liquid-phase xylose conversion. Reprinted with permission from ref. 67. Copyright 2017, ELSEVIER; (b) simplified process of the catalyst synthesis. Reprinted with permission from ref. 68. Copyright 2020, ELSEVIER; (c) proposed mechanism for Meerwein–Ponndorf–Verley (MPV) reduction on zeolite catalysts. Reprinted with permission from ref. 69. Copyright 2017, Royal Society of Chemistry; (d) the proposed reaction mechanism of CaCl<sub>2</sub>·4H<sub>2</sub>O catalyst in IPA/MSH biphasic system. Reprinted with permission from ref. 70. Copyright 2024, Springer Nature.

vacancies accelerate the HDO of these etherified intermediates (Fig. 4f).<sup>51</sup>

As summarized in Table 2, the catalytic efficiency of these integrated catalysts primarily depends on the effective integration of acidic and metallic sites, as well as the regulation of the microenvironment of catalyst. While the hydrophobic catalyst and PMHS strategy offers great selectivity and mild temperatures, the stoichiometric consumption of PMHS faces challenges for industrial scalability. In contrast, MOF-derived catalysts demonstrate superior versatility in handling complex di- and polysaccharides by fine-tuning acid site distributions. However, the potential for pore contraction due to excessive grafting of functional groups remains a concern for mass transfer. In the future, efforts should be directed towards enhancing the design of multifunctional catalysts with improved mass transfer properties and better control over acid site distribution to achieve higher efficiency and robustness in the conversion of complex sugars to valuable furanic compounds.

**3.2.2.2 Pentose-derived furfural conversion.** Similarly, the direct and efficient conversion of pentoses into high-value furanic compounds such as 2-MF and FOL relies on the design of bifunctional integrated catalysts. These catalysts coordinate dehydration and hydrogenation steps while suppressing side reactions, thereby achieving high-selectivity one-pot transformation.

Early research efforts focused on precious metal–solid acid systems, which aimed to synergistically complete the two steps of dehydration (acid sites) and hydrogenation (metal sites). One

example is the sulfuric acid-modified Pt/ZrO<sub>2</sub> catalyst (Pt/ZrO<sub>2</sub>-SO<sub>4</sub>) developed by Fraga *et al.*, in which acidic and metallic sites were integrated on the same surface to enable the direct conversion of xylose to FOL.<sup>67</sup> However, the FOL yield was only 9%, indicating that simple site proximity is insufficient. In this system, isolated acidic or metallic sites preferentially led to furfural or xylitol formation, respectively (Fig. 5a). This observation indicates that effective synergy requires not only spatial adjacency but also a proper balance and accessibility of active sites. To overcome these limitations, the same group subsequently developed a Pt/SBA-15-SO<sub>3</sub>H catalyst, in which uniformly distributed sulfonic acid groups were anchored within the inorganic SBA-15 framework together with noble-metal Pt nanoparticles, resulting in a markedly enhanced FOL yield of 60% (Table 2).<sup>71</sup> This improvement highlights the importance of stabilizing acidic sites and optimizing catalyst architecture to promote efficient dehydration–hydrogenation coupling.

To reduce reliance on noble metals and to modulate hydrogenation pathways, increasing attention has been devoted to non-noble-metal catalysts and alternative hydrogen activation strategies. Deng *et al.* designed a bifunctional Cu/SBA-15-SO<sub>3</sub>H catalyst, in which sulfonic acid groups were incorporated into the SBA-15 *via* a co-condensation method (Fig. 5b).<sup>68</sup> The catalyst demonstrated a FOL yield of 62.6% from xylose in a biphasic H<sub>2</sub>O/*n*-butanol system (Table 2). The mesoporous structure facilitates mass transfer of reactants and intermediates, thereby suppressing side reactions such as xylitol formation and over-hydrogenation. Meanwhile, the biphasic solvent



system enables *in situ* extraction of the produced FOL, effectively shortening its residence time in the acidic phase and enhancing the reaction efficiency. Building on this concept, Fraga and co-workers further explored the involvement of non-metallic sites in hydrogenation reactions and proposed a metal-free catalytic strategy using zeolites (Beta, USY, and ZSM-5) for the tandem conversion of xylose to FOL.<sup>69</sup> In this system, Brønsted acid sites facilitated xylose dehydration to furfural, while framework Al-Lewis centers (generated by hydrolyzed Al-O-Si bonds) catalyzed the subsequent Meerwein-Ponndorf-Verley (MPV) reduction of furfural to FOL, with IPA acting as the hydrogen donor. The Beta zeolite achieved a 75% FOL selectivity, attributed to its unique tetrahedral Al-Lewis configuration and BEA topology, which optimized the six-membered transition state for hydride transfer (Fig. 5c).

A unique innovation involves controlling the reaction pathway to steer product selectivity. Liu and colleagues introduced an IPA/melt salt hydrate (MSH) dual-phase system, where  $\text{CaCl}_2 \cdot 4\text{H}_2\text{O}$  functions as both the solvent and catalyst, yielding 62 mol% of FOL.<sup>70</sup> Notably, no furfural was detected during the conversion, indicating the presence of a new reaction pathway that bypasses furfural as an intermediate, with xylose being converted *via* xylitol to FOL (Fig. 5d). This finding provides a crucial mechanistic insight into the power of solvent and specific catalyst design to dictate the intermediate species and pathway, thereby circumventing the stability and side-reaction issues associated with furfural.

In summary, the direct conversion of pentoses has been explored through metal-acid systems to MOFs and metal-free strategies. Collectively, these studies indicate that the field is moving toward higher product yields, lower catalyst cost, and simplified process integration. The main future challenges focus on achieving precise control over the distance and ratio of acid and metal sites on the nanoscale to maximize the efficiency of tandem reactions and on deep understanding and leveraging the mechanistic modulating capability of novel solvent systems to unlock new, highly selective conversion pathways.

## 4. Conclusion and future challenges

The conversion of saccharides into high-value furanic compounds represents a promising pathway for the sustainable utilization of biomass resources. This review has highlighted the significant progress made in the development of catalytic systems for the one-pot conversion of saccharides into furanic compounds such as DMF, 2-MF, FOL, 5-MF, DMTHF, and HXD. The integration of hydrolysis, dehydration, and hydrogenation reactions into a one-pot catalytic process has demonstrated considerable potential for improving efficiency, reducing energy consumption, and minimizing the complexity of traditional multi-step processes. The incorporation of novel materials such as MOFs, zeolites, and carbon-based supports offers exciting opportunities for improving catalytic performance. Despite the significant progress made in one-pot saccharides to furanic compound conversions, there are still several challenges that remain.

(1) Catalyst design: the development of multifunctional catalysts, particularly those incorporating both acidic and metallic sites, has been a major breakthrough. These catalysts enable the simultaneous dehydration of saccharides and hydrogenation of intermediates, leading to high yields of target furanic compounds. However, challenges remain in optimizing the stability and reusability of these catalysts. For example, leaching of acidic groups (*e.g.*, sulfonic acid groups) from bifunctional catalysts with surface-grafted acidic groups is a common problem, which hinders the long-term use of the catalysts, especially under harsh reaction conditions. Therefore, enhancing the stability of acidic groups is crucial for ensuring the practicality of these catalysts in large-scale applications.

(2) Substrate scope: while significant progress has been made in converting simple sugars like fructose and glucose, the direct conversion of disaccharides and polysaccharides such as cellulose and hemicellulose to furanic compounds has still not been fully explored, and the yields are generally quite low. The complex depolymerization of polysaccharides to monosaccharides are often a limiting step in these processes. Advances in catalyst design and reaction engineering are needed to expand the substrate scope and improve the overall efficiency of these processes.

(3) Reaction solvents: the choice of solvent and reaction medium plays a crucial role in the efficiency of saccharide conversion. Biphasic systems, ionic liquids, and supercritical fluids have shown promise in enhancing reaction selectivity and product separation. Future research should focus on developing more environmentally friendly and cost-effective solvents to further improve the sustainability of these processes.

## Author contributions

X. Cheng and M. Dong wrote the original draft. H. Liu and B. Han supervised the review and revised the manuscript. All authors revised and finalized the manuscript.

## Conflicts of interest

There are no conflicts to declare.

## Data availability

No primary research results, software or code have been included and no new data were generated or analysed as part of this review.

## Acknowledgements

This work was supported by startup funding from Zhengzhou University.

## Notes and references

- 1 N. Abas, A. Kalair and N. Khan, *Futures*, 2015, **69**, 31–49.
- 2 M. Huang and P. Zhai, *Adv. Clim. Change Res.*, 2021, **12**, 281–286.



- 3 J. Wang, J. Fu, Z. Zhao, L. Bing, F. Xi, F. Wang, J. Dong, S. Wang, G. Lin, Y. Yin and Q. Hu, *Innovation*, 2023, **4**, 100423.
- 4 D. M. Alonso, S. G. Wettstein and J. A. Dumesic, *Chem. Soc. Rev.*, 2012, **41**, 8075–8098.
- 5 D. Carpenter, T. L. Westover, S. Czernik and W. Jablonski, *Green Chem.*, 2014, **16**, 384–406.
- 6 Y. Wu, J. Zhou, E. Li, M. Wang, K. Jie, H. Zhu and F. Huang, *J. Am. Chem. Soc.*, 2020, **142**, 19722–19730.
- 7 C. Jiang, C. Wang, H. Xu, H. Liu and X. Ma, *Fuel*, 2021, **285**, 119113.
- 8 O. Simoska, Z. Rhodes, S. Weliwatte, J. R. Cabrera-Pardo, E. M. Gaffney, K. Lim and S. D. Minter, *ChemSusChem*, 2021, **14**, 1674–1686.
- 9 Y. Zhong, H. Frost, M. Bustamante, S. Li, Y. S. Liu and W. Liao, *Renew. Sustain. Energy Rev.*, 2020, **121**, 109675.
- 10 G. Zang, A. Shah and C. Wan, *J. Clean. Prod.*, 2020, **260**, 120837.
- 11 Y. J. Pagán-Torres, T. Wang, J. M. R. Gallo, B. H. Shanks and J. A. Dumesic, *ACS Catal.*, 2012, **2**, 930–934.
- 12 K. R. Enslow and A. T. Bell, *ChemCatChem*, 2015, **7**, 479–489.
- 13 L. Zhang, H. Yu, P. Wang and Y. Li, *Bioresour. Technol.*, 2014, **151**, 355–360.
- 14 Y. Yang, C. Hu and M. M. Abu-Omar, *J. Mol. Catal. A: Chem.*, 2013, **376**, 98–102.
- 15 D. Weidener, W. Leitner, P. Domínguez de María, H. Klose and P. M. Grande, *ChemSusChem*, 2021, **14**, 909–916.
- 16 T. D. Swift, H. Nguyen, A. Anderko, V. Nikolakis and D. G. Vlachos, *Green Chem.*, 2015, **17**, 4725–4735.
- 17 J. Wang, W. Xu, J. Ren, X. Liu, G. Lu and Y. Wang, *Green Chem.*, 2011, **13**, 2678–2681.
- 18 L. Zhang, G. Xi, Z. Chen, Z. Qi and X. Wang, *Chem. Eng. J.*, 2017, **307**, 877–883.
- 19 N. Zhou, C. Zhang, Y. Cao, J. Zhan, J. Fan, J. H. Clark and S. Zhang, *J. Clean. Prod.*, 2021, **311**, 127780.
- 20 X. Xing, R. Hu, W. Liu, X. Shi, G. Lyu, H. Gao and S. Xu, *Green Chem.*, 2025, **27**, 10823–10836.
- 21 S. Körner, J. Albert and C. Held, *Front. Chem.*, 2019, **7**, 661.
- 22 X. Zhang, H. Lu, K. Wu, Y. Liu, J. Wu, Y. Zhu and B. Liang, *Renewable Energy*, 2024, **233**, 121144.
- 23 J. Shi, H. Gao, Y. Xia, W. Li, H. Wang and C. Zheng, *RSC Adv.*, 2013, **3**, 7782–7790.
- 24 M. P. Papajewski, S. Nisar, C. Zhang, J. P. Hallett and J. Albert, *RSC Adv.*, 2025, **15**, 14259–14263.
- 25 B. M. Matsagar, S. A. Hossain, T. Islam, H. R. Alamri, Z. A. Allothman, Y. Yamauchi, P. L. Dhepe and K. C.-W. Wu, *Sci. Rep.*, 2017, **7**, 13508.
- 26 L. Lin, Y. Zeng, S. Zhang, D. Hu, Z. Jiang, G. Guan and K. Yan, *Appl. Catal., B*, 2025, **361**, 124592.
- 27 X. Liao, H. Cui, H. Luo, Y. Lv and P. Liu, *Chem. Eng. J.*, 2025, **503**, 158336.
- 28 J. Chen, R. Liu, Y. Guo, L. Chen and H. Gao, *ACS Catal.*, 2015, **5**, 722–733.
- 29 G. Gao, J. Remón, Z. Jiang, L. Yao and C. Hu, *Appl. Catal., B*, 2022, **309**, 121260.
- 30 N. S. Date, A. M. Hengne, K.-W. Huang, R. C. Chikate and C. V. Rode, *Green Chem.*, 2018, **20**, 2027–2037.
- 31 W. Lin, Y. Chen, Y. Zhang, Y. Zhang, J. Wang, L. Wang, C. C. Xu and R. Nie, *ACS Catal.*, 2023, **13**, 11256–11267.
- 32 Z. Zhao, C. Yang, P. Sun, G. Gao, Q. Liu, Z. Huang and F. Li, *ACS Catal.*, 2023, **13**, 5170–5193.
- 33 M. Sherbi, M. Stuckart and J. Albert, *Biofuels, Bioprod. Biorefin.*, 2021, **15**, 1431–1446.
- 34 Y. Román-Leshkov, C. J. Barrett, Z. Y. Liu and J. A. Dumesic, *Nature*, 2007, **447**, 982–985.
- 35 L. Hu, X. Tang, J. Xu, Z. Wu, L. Lin and S. Liu, *Ind. Eng. Chem. Res.*, 2014, **53**, 3056–3064.
- 36 X. Cheng, Y. Xin, Y. Liu, S. Luan, M. Dong, T. Wang, L. Zhang, B. Zhang, B. Chen, H. Liu and B. Han, *ACS Sustainable Chem. Eng.*, 2024, **12**, 11980–11986.
- 37 X. Chen, R. Li, Y. Zhong, H. Liu, D. Hu and C. Liang, *Chem. Eng. J.*, 2024, **499**, 155854.
- 38 H. Li, X. Nie, H. Du, Y. Zhao, J. Mu and Z. C. Zhang, *ChemSusChem*, 2023, **17**, e202300880.
- 39 M. Braun and M. Antonietti, *Green Chem.*, 2017, **19**, 3813–3819.
- 40 P. P. Upare, D. W. Hwang, Y. K. Hwang, U.-H. Lee, D.-Y. Hong and J.-S. Chang, *Green Chem.*, 2015, **17**, 3310–3313.
- 41 T. Thananathanachon and T. B. Rauchfuss, *Angew. Chem., Int. Ed.*, 2010, **49**, 6616–6618.
- 42 T. Li, S. S. G. Ong, J. Zhang, C. Jia, J. Sun, Y. Wang and H. Lin, *Catal. Today*, 2020, **339**, 296–304.
- 43 N. Shi, T. Zhu, H. Zhang, H. Huang, L. Zhou, Y. Liu and R. Shu, *ACS Omega*, 2023, **8**, 11574–11582.
- 44 Y. Liu, J. Long, Z. Huang, L. Chen, C. Wang, X. Zhang and L. Ma, *Biomass Bioenergy*, 2024, **190**, 107405.
- 45 J. Xu, X. Miao, L. Liu, Y. Wang and W. Yang, *ChemSusChem*, 2021, **14**, 5311–5319.
- 46 Z. Wei, J. Lou, Z. Li and Y. Liu, *Catal. Sci. Technol.*, 2016, **6**, 6217–6225.
- 47 R. Insyani, D. Verma, S. M. Kim and J. Kim, *Green Chem.*, 2017, **19**, 2482–2490.
- 48 R. Insyani, D. Verma, H. S. Cahyadi, S. M. Kim, S. K. Kim, N. Karanwal and J. Kim, *Appl. Catal., B*, 2019, **243**, 337–354.
- 49 Q. Deng, X. Hou, Y. Zhong, J. Zhu, J. Wang, J. Cai, Z. Zeng, J.-J. Zou, S. Deng, T. Yoskamtorn and S. C. E. Tsang, *Angew. Chem., Int. Ed.*, 2022, **61**, e202205453.
- 50 M. A. Jackson, M. Appell and J. A. Blackburn, *Ind. Eng. Chem. Res.*, 2015, **54**, 7059–7066.
- 51 D. Verma, R. Insyani, R. Gilang Kurniawan, H. Jo, L. Hakeem and J. Kim, *Chem. Eng. J.*, 2024, **496**, 153696.
- 52 C. V. Nguyen, J.-Y. Yeh, T. V. Tran and K. C.-W. Wu, *Green Chem.*, 2022, **24**, 5070–5076.
- 53 C. Zhu, H. Wang, C. Cai, K. Bi, B. Cai, X. Song, Q. Liu and L. Ma, *ACS Sustainable Chem. Eng.*, 2019, **7**, 16026–16040.
- 54 K. I. Galkin and V. P. Ananikov, *ChemSusChem*, 2019, **12**, 185–189.
- 55 W. Yang, M. R. Grochowski and A. Sen, *ChemSusChem*, 2012, **5**, 1218–1222.
- 56 M. R. Grochowski, W. Yang and A. Sen, *Chem.–Eur. J.*, 2012, **18**, 12363–12371.
- 57 R. F. Perez and M. A. Fraga, *Green Chem.*, 2014, **16**, 3942–3950.



- 58 L. Xu, R. Nie, H. Xu, X. Chen, Y. Li and X. Lu, *Ind. Eng. Chem. Res.*, 2020, **59**, 2754–2760.
- 59 J. Lessard, J.-F. Morin, J.-F. Wehrung, D. Magnin and E. Chornet, *Top. Catal.*, 2010, **53**, 1231–1234.
- 60 J. Cui, J. Tan, X. Cui, Y. Zhu, T. Deng, G. Ding and Y. Li, *ChemSusChem*, 2016, **9**, 1259–1262.
- 61 H. Li, H. Liu, C. Cai, H. Wang, Y. Huang, S. Li, B. Yang, C. Wang, Y. Liao and L. Ma, *Catal. Commun.*, 2023, **175**, 106625.
- 62 H. Li, W. Zhao, A. Riisager, S. Saravanamurugan, Z. Wang, Z. Fang and S. Yang, *Green Chem.*, 2017, **19**, 2101–2106.
- 63 X. Hou, Y. Zhong, J. Xiao, J. Wang, J. Cai, Z. Zeng, S. Deng and Q. Deng, *AIChE J.*, 2023, **69**, e18047.
- 64 H. Li, W. Zhao and Z. Fang, *Appl. Catal., B*, 2017, **215**, 18–27.
- 65 K. Ji, C. Shen, J. Yin, X. Feng, H. Lei, Y. Chen, N. Cai and T. Tan, *Ind. Eng. Chem. Res.*, 2019, **58**, 10844–10854.
- 66 J. Li, Z. Song, Y. Hou, Z. Li, C. Xu, C.-L. Liu and W.-S. Dong, *ACS Appl. Mater. Interfaces*, 2019, **11**, 12481–12491.
- 67 R. F. Perez, S. J. Canhaci, L. E. P. Borges and M. A. Fraga, *Catal. Today*, 2017, **289**, 273–279.
- 68 T. Deng, G. Xu and Y. Fu, *Chin. J. Catal.*, 2020, **41**, 404–414.
- 69 P. N. Paulino, R. F. Perez, N. G. Figueiredo and M. A. Fraga, *Green Chem.*, 2017, **19**, 3759–3763.
- 70 D. Liu, Z. Wen, C. Yang, P. Wei, Z. Zhang and Q. Li, *Cellulose*, 2024, **32**, 827–837.
- 71 S. J. Canhaci, R. F. Perez, L. E. P. Borges and M. A. Fraga, *Appl. Catal., B*, 2017, **207**, 279–285.

